

**Irankuh lead-zinc mining district, southern Isfahan, Iran:
Evidences of geology, fluid inclusion and isotope geochemistry**Abbas Esmaili Sevieri ¹, Mohammad Hassan Karimpour ^{2,*},
Azadeh Malekzadeh Shafaroudi ², Asadollah Mahboubi ¹, Yucai Song ³¹ Department of Geology, Faculty of Science, Ferdowsi University of Mashhad, Mashhad, Iran² Department of Geology and Research Center for Ore Deposit of Eastern Iran, Faculty of Science,
Ferdowsi University of Mashhad, Mashhad, Iran³ Institute of Geology, Chinese Academy of Geological Sciences, Beijing, China**ARTICLE INFO**

Submitted: March 2019

Accepted: June 2019

Available on line: July 2019

* Corresponding author:

karimpur@um.ac.ir

DOI: 10.2451/2019PM867

How to cite this article:

Esmaili Sevieri A. et al. (2019)

Period. Mineral. 88, 277-296

ABSTRACT

Irankuh mining district is one of the most important Pb-Zn MVT-type mineralization, which is located in Malayer-Isfahan Metallogenic Belt (MIMB), Western Iran. The deposits are hosted by Cretaceous dolostone and minor Jurassic shale. Hydrothermal alteration minerals are composed of dolomite, Fe-rich dolomite, ankerite, and minor quartz. Hypogene minerals are sphalerite, galena, and bitumen associated with minor pyrite, chalcopyrite, and barite. The paragenesis, alteration, shape, and dimension of mineralization are different in the two host rocks. Microthermometric data reveal the ore-forming fluids are medium-to-low temperature (188-280°C) and medium-salinity (7.5 to 20.5 wt% NaCl equivalents). The possible source of sulfur ($\delta^{34}\text{S} = -1.8$ to $+0.7\text{‰}$) may be sulfide-bearing sedimentary rocks. However, the S isotope values cannot show a particular source. Very low radiogenic Pb isotopes ($^{206}\text{Pb}/^{204}\text{Pb} = 18.419-18.476$, $^{207}\text{Pb}/^{204}\text{Pb} = 15.634-15.663$, $^{208}\text{Pb}/^{204}\text{Pb} = 38.562-38.670$) indicate that Pb-isotopes had an oceanic slab source and were slightly contaminated by the basement rocks. The hydrothermal fluid originated from the dehydration of Neo-Tethys oceanic subduction slab (forearc area), which is MgO-rich and low SiO₂, migrated upward through deep-seated thrust faults from the basement to shallow depths. The Irankuh are similar to MVT deposits based on host rock, epigenetic form, alteration, structure, mineralization, isotope geochemistry and nature of ore-forming fluids.

Keywords: Ore-forming fluid; Sulphur isotope; Lead isotopes; MVT; Irankuh; Iran.

INTRODUCTION

Mississippi Valley-Type (MVT) deposits are epigenetic, stratabound zinc and lead deposits with minor copper hosted by dolostone, limestone, and locally sandstone in platform carbonate sequences inboard of major orogenic belts. The deposits occur mainly as open-space fillings, collapse breccias, and/or as replacement of the carbonate host rock (Leach and Sangster, 1993; Leach et al., 2010). The most (though not all) MVT deposits were produced by enormous fluid systems that migrated through foreland

basins, driven by gravity from an adjacent orogenic belt (e.g. Garven, 1985; Ge and Garven, 1992; Appold and Garven, 1999; Leach et al., 2001). However, some forelands are rich in MVT deposits, whereas others are barren, and this may be due to differences in foreland basins or other factors controlling MVT mineralization worldwide. Leach et al. (2005 and 2010) and He et al. (2009) suggested the source of the metals can be from basement rocks. In almost all MVT deposits, dolomite alteration and open space filling suggest that the

hydrothermal fluids were rich in Mg (Kesler and Carrigan, 2002; Leach et al., 2005, 2010; He et al., 2009; Karimpour et al., 2018).

The geology, tectonic style and spatial mineral occurrence of Iran is highly influenced by the development and history of the Tethyan region. The tectonic events, which occurred around the Iranian Plate margins, are related to rifting processes of Gondwana and subsequent collision with the Arabian plate from the WSW. These important processes affected the Iranian Plate and the adjacent plates, such as the African, Indian, Arabian, and Eurasian Plates, during Mesozoic to Tertiary times (Alavi, 2004). The Tethyan region, which includes the Iranian Plate and the adjacent areas, underwent three major evolutionary stages. The first stage was the closing of the Paleo-Tethys and rifting of the Neo-Tethys from early Permian to late Triassic times. With the second stage, the subduction process of the Neo-Tethys and the collision of the Indian Plate with the Eurasian Plate from the Jurassic to the early Lower Tertiary began. The third and last stage is associated with the collision between the Arabian plate and the Eurasian plate from early Tertiary to the present (Shufeng et al., 2002).

Iran has about 600 Zn-Pb deposits and occurrences (Ghorbani, 2002). Based on the spatial occurrences of Zn-Pb deposits of Iran relative to the tectonic structures, four important metallogenic provinces in Iran, such as the Central Alborz Metallogenic Belt (CAMB), Malayer-Isfahan Metallogenic Belt (MIMB), Yazd-Anarak Metallogenic Belt (YAMB), and Tabas-Posht-e-Badam Metallogenic Belt (TPMB), has been demonstrated (Rajabi et al., 2012) (Figure 1). The MIMB, with 200 km long and 100 km wide, contains more than 200 Zn-Pb ore occurrences and some major deposits, which Irankuh mining district is the most important of them (Figure 1). The MIMB is located in the central part of the Sanandaj-Sirjan Zone (SSZ). The development of the SSZ is related to the generation of the Neo-Tethys Ocean in the Permian and its subsequent destruction due to the convergence and continental collision between the Arabian and Iran plates during Cretaceous to Tertiary time (Mohajjel et al., 2003; Agard et al., 2005; Ghasemi and Talbot, 2005). Recent studies show that the SSZ was formed by the accretion of several Triassic to Cretaceous magmatic arcs (Arvin et al., 2007; Khalaji et al., 2007). The large Zagros thrust zone (ZTZ, Figure 1), located between the SSZ and the Zagros ranges, is generally considered to constitute the suture between the Arabian plate and the Iran plate (Golonka, 2004; Agard et al., 2005). Based on detrital zircon ages, Horton et al. (2008) suggested that this collision occurred between the middle Eocene and the late Oligocene.

Based on the lithology of ore-bearing strata (Momenzadeh,

1976; Rastad, 1981; Modaberi, 1994) sediment-hosted Zn-Pb deposits of the MIMB are restricted to three main stratigraphic positions: 1) the Jurassic ore-bearing horizon that includes sandstone-hosted deposits at the top of the Shemshak shales and sandstones; 2) the Cretaceous ore-bearing horizon that has sandy and silty dolomites at the base and grades to massive limestones to the top; and 3) the Cretaceous ore-bearing horizon, corresponding to interlayered shales and siliceous dolomitic limestones (Rajabi et al., 2012). About 50% of the known Zn-Pb mineralization's of the MIMB occur in the second item ore-bearing horizon of the Cretaceous sequence.

The Irankuh mining district located about 20 km southwestern Isfahan, between longitudes 51°32" and 51°41", and latitudes 32°27" and 32°33", Iran. The north of Irankuh mining district includes 3 cluster deposits (Gushfil, Blind, Tapeh Sorkh and Kolahdarvazeh; Figure 2) and 5 prospect areas (zone-1 to 5 of Romarmar, Figure 2), that Romarmar five zone is the most important prospect area, hosted mostly by Cretaceous carbonate sequence and to a lesser extent by clastic sediments, Jurassic in age, with total reserve of 13.5 Mt ores at 4% Zn and 2% Pb (Karimpour et al., 2018). Both underground and open pit mining in the Irankuh district have started since 1952. The deposits such as Gushfil and Tapeh Sorkh, which considered as old mines in the district, have been mined out as open cast to certain economic viable depths, respectively 180 meters and 80 meters. The mining operation continued using underground mining to further depths as in Gushfil, the lowest level of underground mining reached 380 meters down the surface. The 3D model of the Tapeh Sorkh reserve shows the minable ore extends to 135 meters down the surface. In the light of discoveries of new deposits, the mines such as Roarmarmar five zone and Gushfil one zone are in the production line using underground long wall method.

Many scholars have studied the geology of old mines as Gushfil and Tapeh Sorkh and Kolahdarvazeh (Rastad, 1981; Ghazban et al., 1994; Ghasemi, 1995; Reichert, 2007; Hosseini-Dinani et al., 2015; Hosseini-Dinani and Aftabi, 2016; Boveiri-Konari et al., 2017; Saboori et al., 2019) but other deposits such as the Romarmar five zone and the Blind, which discovered in last decade, less reviewed. Therefore, a comprehensive detail survey to study all the geological package of the district seems to be inevitable. In the last two years, a comprehensive detail survey includes field geology, ore microscopy, fluid inclusion microthermometry, geochemistry of galena and sphalerite, and the sulphur and lead isotopic composition have been carried out. Part of the results mostly on geochemistry of galena and sphalerite and delineating the tectonic settings of

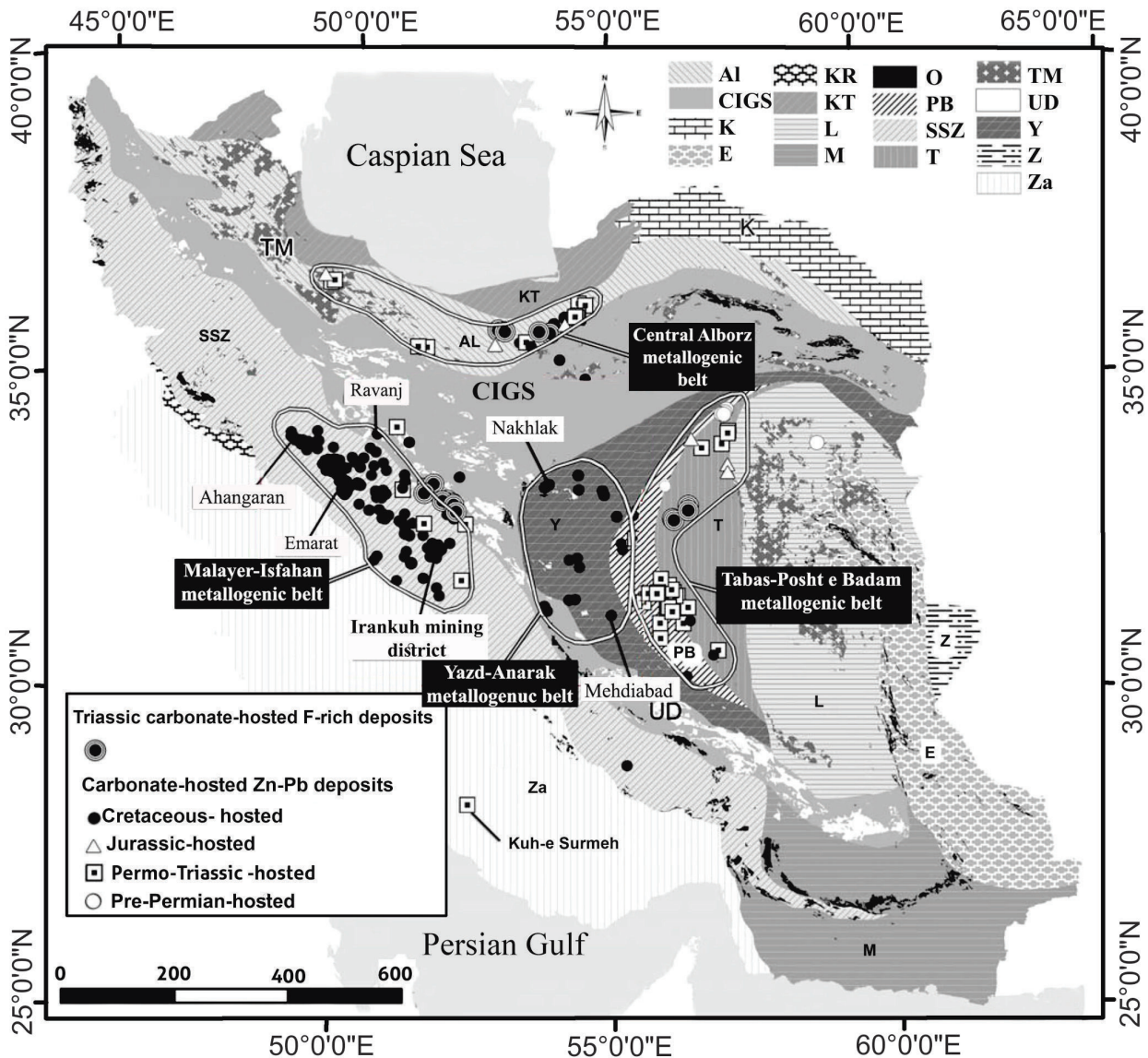


Figure 1. Distribution map of carbonate-hosted Zn-Pb and F-rich deposits according to the age of host rocks in the CAMB, TPMB, MEMB, and YAMB. AI, Alborz ranges; CIGS, Central Iranian geological and structural gradual zone; E, East Iran ranges; K, Kopeh-Dagh; KR, Kermanshah Radiolarites subzone; KT, Khazar-Talesh-Ziveh structural zone; L, Lut block; M, Makran zone; O, ophiolite belts; PB, Posht-e-Badam block; SSZ, Sanandaj-Sirjan zone; T, Tabas block; TM, tertiary magmatic rocks; UD, Urumieh-Dokhtar magmatic arc; Y, Yazd block; Z, Zabol area; Za, Zagros ranges. Adopted from Rajabi et al. (2012).

area has been published earlier (Karimpour et al., 2018; Karimpour and Sadeghi, 2018; Karimpour et al., 2019). The current study provides the results on ore microscopy, fluid inclusion microthermometry of sphalerite and sparry dolomite, the sulfur isotopic composition of galena and sphalerite samples, and Pb isotopes of galena, which led to a genetic model of zinc and lead deposits of the Irankuh mining district.

GEOLOGICAL SETTING

The late Triassic to late Jurassic tensional regime in many parts of Iran provides a shallow sedimentary basin to deposition of thick sequences of molasses and came to an end during the late Jurassic (140 Ma) compressional movements. The sea regressed from many parts of Central and northern Iran and many continental areas emerged. The boundary of the Jurassic and Cretaceous system is generally marked by an unconformity, significant hiatus,

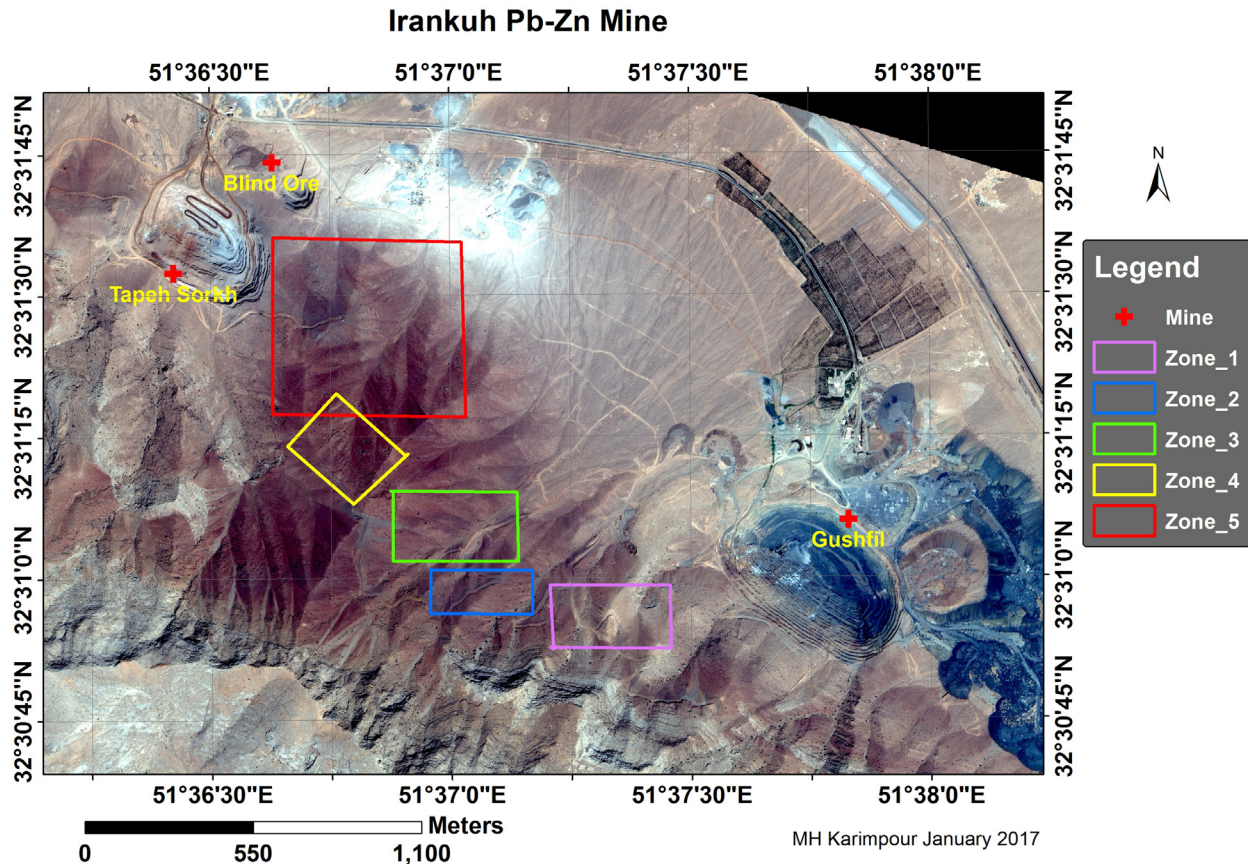


Figure 2. Location map of Gushfil, Tapeh Sorkh, and Blind deposits associated with zone-1 to 5 of Romarmar prospect area in the Irankuh mining district.

or red continental detritus as basal conglomerate and evaporitic sediments (Berberian and King, 1981). The Cretaceous period coincided with a protracted magmatic quiescence and deposition of anomalous thicknesses of Barremian to Aptian carbonates that suggests the presence of pull-apart basins along the SSZ (Şengör, 1990). Part of the Cretaceous carbonate sequence hosts three cluster deposit and prospect areas in north Irankuh mining district.

Two main geological formation exposed in the mining area (Figure 3): 1) Jurassic shale, partly organic rich, with interbedded sandstone, equivalent with the Shemshak group. 2) The Cretaceous dolostone and limestone with a thickness about 1000 meter (Karimpour and Sadeghi, 2018). In contrary to Zahedi (1976) and Rastad (1981) studies, there is no evidence of a basal conglomerate of the Cretaceous sequence on the surface outcrop in the Irankuh. But basal conglomerate composed of rounded quartz grains and plagioclase components in a fine rich iron oxide matrix is found sporadically only in few drill

cores, which while passing through carbonate sequence has reached down to basement shales. The Jurassic shale and sandstone are thrust over the Cretaceous carbonate. Six lithostratigraphic units including dolostone and interbedded limestone units were mapped in the area, which the thick bedded dolostone unit host all of known deposits in the Irankuh mining district (Figure 3). Dolostone units had sufficient porosity to serve as a favorable host rock. Karimpour et al. (2018) suggested the thrust-reverse faults with trending about N85°E were very important for the formation Irankuh Pb-Zn deposits. The strike-slip faults with trending N30°-45°E are considered as destructive types, because they displaced the mineralization (Figure 3).

SAMPLING AND ANALYTICAL METHODS

Ore mineralogy

Sixty-five polished and thin-polished sections were collected from surface (open pit), drill holes, and from various levels of tunnels in the ore-bearing vein in the

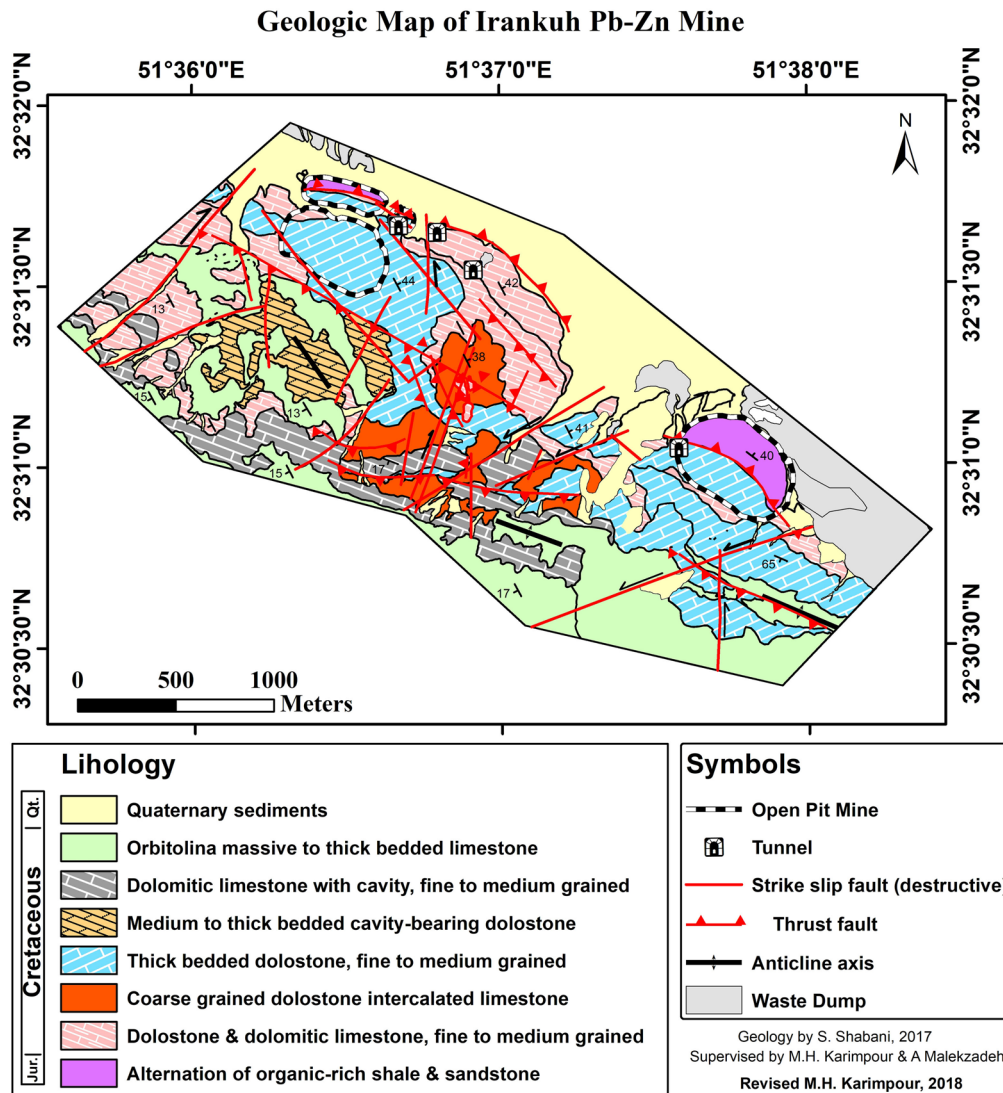


Figure 3. Geological map of Irankuh mining district (Karimpour and Sadeghi, 2018).

Gushfil, Gushfil one zone, Romarmar five zone, Tapeh Sorkh and Blind deposits. The samples were selected in such a way as to show all the veins with different host rock.

Fluid inclusion

The fluid inclusion samples were collected from surface, drill holes, and from various levels of tunnels in the mineralized zone of the Gushfil, Romarmar five zone, Tapeh Sorkh and Blind deposits. Twenty doubly polished wafers (150 μm thick) (sphalerite and dolomite wafers coexisting with sphalerite and galena) were processed for microthermometric analysis to gain preliminary feedback on the temperatures and salinities of the ore-forming fluid. To distinguish shape, size, phase, distribution pattern and

possible origin of fluid inclusions, polished thin sections were checked under transmitted light.

Microthermometric measurements were organized using standard techniques (Roedder, 1972, 1984) and a Linkam THM 600 heating-freezing stage (-190 to 600 °C) affixed on an Olympus TH4-200 microscope stage at Ferdowsi University of Mashhad, Iran. The accuracy is estimated to be ±0.2 °C on freezing, ±2 °C below 350 °C and approximately ±4 above 350 °C on heating. The stage was calibrated at low temperatures with the aid of heptane (-90.6 °C), chloroform (-63.0 °C), chlorobenzene (-45.6 °C), n-dodecane (-9.6 °C) and distilled water (0.0 °C). Calibration at 45 °C was undertaken via Merck Melting Point standard 9645 and at 306 °C via sodium nitrate.

Sulfur isotopes

In the Irankuh mining district, sphalerite and galena are the two appropriate sulfide minerals for isotopic analysis because the amount of sulfur and its microscopic features were suitable. For interpreting the origin and the genesis model of the deposits, the $\delta^{34}\text{S}$ of sphalerite and galena samples were analysed.

The galena- and sphalerite-bearing samples that were selected for fluid inclusion study and sulfur isotopic analysis show a close relationship with dolomite. Therefore, we can use the measured microthermometric temperature of dolomite for galena and/or sphalerite or microthermometric temperature of sphalerite mineral for galena and itself. Fourteen samples were collected from drill holes, open pits and underground levels. The samples were crushed and homogenized. The samples were crushed again in a ceramic mortar and then sieved into four standard sieves with mesh numbers of 10, 16, 18, and 20. Samples with mesh numbers between 18 and 20, which have the most frequent fractions (1 to 0.850 mm), were selected, and the high purity concentrations of sphalerite and galena were handpicked under a binocular microscope.

Isotopic analyses of sulfur for galena and sphalerite samples were performed at Beijing Geological Institute of Nuclear Industry, China. These measurements were performed by Delta V plus gas isotope mass spectrometer. GBW 04415 and GBW 04414 Ag_2S were used as the external standards. The results ($\delta^{34}\text{S}$ values) are represented in the standard per mil notation relative to the international Canyon Diablo Troilite (CDT) standard. The analytical accuracy was 0.2‰.

Lead isotopes

Six galena samples were selected from the veins. The mineral samples were ground to a ~200 mesh size for chemical dissolution. The Pb isotopic analyses of the galena samples were conducted at the Institute of Geology, Chinese Academy of Geological Sciences, Beijing, China. The samples were dissolved in 3 ml HF and 1 ml HNO_3 and then dried. The residues were dissolved in HBr and then loaded onto an ion exchange column (AG1-X8) to derive PbCl_2 of high purity. The Pb isotopes were analyzed using a Nu Plasma HR MC-ICPMS, using a TI doping technique (He et al., 2005). Analytical errors are less than 0.05% for $^{206}\text{Pb}/^{204}\text{Pb}$, $^{207}\text{Pb}/^{204}\text{Pb}$, and $^{208}\text{Pb}/^{204}\text{Pb}$ ratios.

ORE DEPOSITS GEOLOGY

The Zn-Pb mineralization in northern Irankuh mining district occurred as veins and veinlets. All of the deposits and prospect areas control by faulting parallel to Zagros orogenic belt, in an azimuth of

310-330°. The deposits such as Gushfil and Blind dipping to NE that the dip value varied from 60° to 80°. The deposits such as Tapeh Sorkh and Romarmar five zone dipping to SW and the dip value mostly is 35-50°. There is an exception in the Romarmar five zone, which only a single vein mostly containing galena show the dip value of 60° to the SW.

The sulphide mineralogy as other MVT deposits throughout the world are simple (Leach et al., 2010), consists mainly sphalerite, galena, and pyrite. The gangue minerals are principally dolomite with minor quartz, barite, and calcite. Finally, widespread weathering influenced the superficial levels of the area covering the alteration of the host-rocks. A supergenic stage consisting of secondary minerals (malachite, hematite, goethite, smithsonite, cerussite, and anglesite) was formed during the weathering and oxidation of the ore.

Texture

Deposition of ores in the Irankuh district, like other MVT districts throughout the world, involve an inextricable link between sulfide precipitation, host rock replacement and dissolution, open space filling, and solution collapse of the host rocks. This interrelationship exists because sulfide precipitation is nearly always an acid generating process (Anderson, 1983).

The sulfide replacement of the carbonate rocks is the most important type of ore occurrence, accounting for about 60 percent of total resources of metal. The remaining ore occurs within dissolution collapse breccias and open-space fillings in fractures and in a variety of vuggy porosity related to dissolution of the host rocks.

Mineralization occurs within dolostone units where it is principally deposited as replacements of dolostone; with some open space filling in tectonic and solution breccia. Minor mineralization occurs in Jurassic shale and sandstone as stockwork veinlets. Mineralization also filled fractures and joints near major thrust faults (Karimpour et al., 2018). Zn-Pb mineralization is found wherever faults cut the dolostone, but the greatest Zn-Pb tonnages and highest ore grades are related to intersections of major faults and the coarse grain dolostone with a favorable chemical composition (Karimpour and Sadeghi, 2018).

Ore mineralogy

The common mineralization consists of sphalerite, galena, bitumen, Fe-rich dolomite, minor pyrite, quartz, and barite. Karimpour and Sadeghi (2018) and Karimpour et al. (2019) suggested that dolostone and shale-sandstone host rocks control the mineral paragenesis of the ore deposit. Shale and sandstone released more silica, so that silicification is associated with these units. Within shale,

the iron minerals such as chlorite reacted with sulfur in solution in to precipitate pyrite. Hydrothermal dolomites in shale host rock are low-Fe. But the behaviour of the iron was quite different in the dolostone. Due to the very low sulfur fugacity, Fe-rich dolomite and in some places ankerite was formed (>8% iron). The iron had a preference and tendency to react with dolomite within dolostone or to be co-precipitated with Mg. Most of the pyrite is associated with shale; Fe-rich dolomite and ankerite are associated with dolostone. Organic rich material (bitumen) is present both in dolostone and shale. At an early stage of mineralization, the hydrothermal fluid apparently remobilized some of the bitumen from Jurassic shale to be redeposited. Displacement along the bitumen zones is very common. At earlier stages, hydrothermal fluid had reduced condition and later it became oxidizing (Karimpour and Sadeghi, 2018).

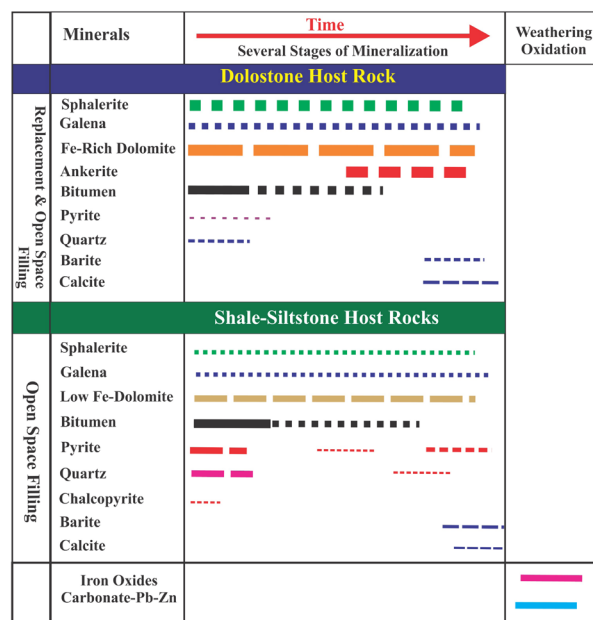
The position of the water table and its changes, host rock lithology, primary mineralogy, fluid access and its chemistry, and climatic regime are the main factors that influenced the supergene processes (Hitzman et al., 2003). Fractures are very abundant in the Irankuh deposits host rock, and therefore the supergene environment is an open system. Therefore, water can continuously reach equilibrium with the atmosphere; in addition, because of the warm and dry climate, biological activities in soil are low, and pH is particularly influenced by host-rock and mineral composition. In the supergene zone, smithsonite, cerussite, anglesite, hematite, and goethite, manganese oxides and to lesser extent malachite are seen. The mineral paragenesis of Irankuh Pb-Zn deposits is shown in Figure 4. In Figure 5, the style of mineralization and some of the common minerals are shown.

FLUID INCLUSIONS

Petrography of fluid inclusions

Petrographic studies of fluid inclusions in sphalerite and hydrothermal dolomite were conducted to identify the hydrothermal fluids and decipher fluid evolution processes. The samples were dominated by primary fluid inclusions (with minor secondary fluid inclusions) that are interpreted as representing the fluids present at the time of hydrothermal mineral growth. The key attributes used to determine primary fluid inclusions were (1) isolation from other inclusions, (2) the random distribution of inclusions (not on planar features), and (3) inclusions that typically follow growth zones. These primary fluid inclusions were defined by trapping during crystal growth, but the secondary inclusions occurred as fracture-controlled arrays after the growth of the host crystal (Roedder, 1984; Van den Kerkhof and Hein, 2001).

Most of the inclusions are small (5-14 μm) in both



MHK 2018

Figure 4. Mineral paragenesis of Irankuh Pb-Zn mining district (after Karimpour et al., 2018). Dashed lines represent intermittent deposition and solid lines show continuous deposition.

sphalerite and hydrothermal dolomite minerals (Table 1). Fluid inclusion shapes include elliptical, round, irregular, and some directional elongated. Fluid inclusions were distributed as clusters, single inclusions, linear arrays, and along fractures or grain boundaries (Figure 6).

At room temperature, all of the measured inclusions are considered primary because they are confined within specific growth zones of the host mineral (Roedder, 1984). The type of inclusions in host minerals are two-phase, liquid-rich with a 5-20% vapour in volume percentage inclusions that homogenize into a liquid state upon heating (Figure 6). The absence of liquid CO₂ or clathrate formation during freezing experiments suggests that none of the inclusions contained significant quantities of CO₂. Although many measurements were achieved, no fluid inclusion evidence for a fluid boiling process in the Irankuh samples was observed because FI along growth zones, FI trapped at the same time, all show equal volumetric phase ratios (Bodnar, 2003).

Microthermometric data

Microthermometric measurements were undertaken on the primary two-phase (L-V) inclusions larger than 5 μm in diameter. Only heating analysis was performed on the inclusions that were very small. Homogenization temperatures (T_h) values range from 193 to 280 °C (average 246.6 °C, n=255) in sphalerite and 188 to 228

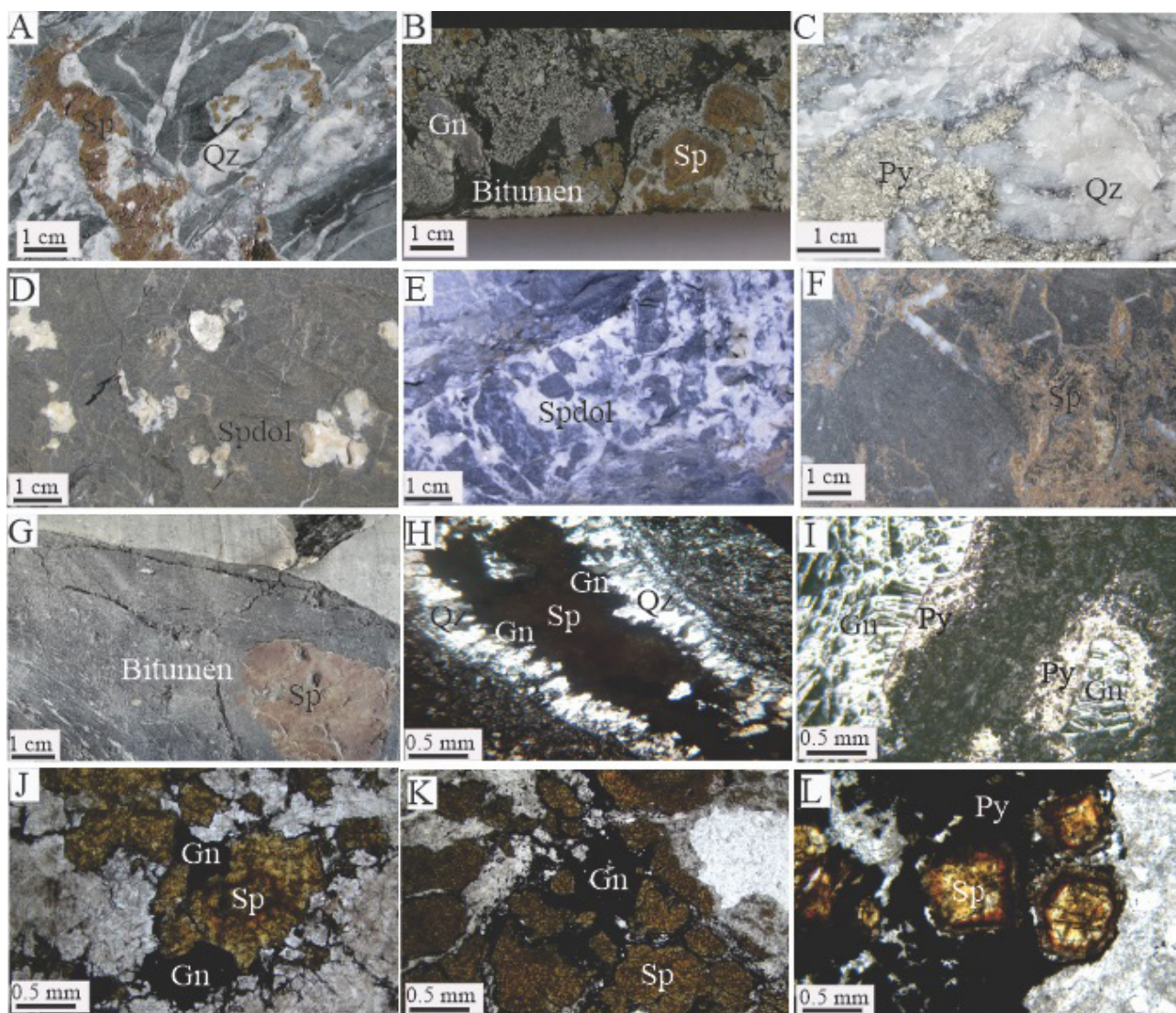


Figure 5. Photographs illustrating the different textures and mineral assemblages of the Irankuh mining district. A) quartz-sphalerite veinlet in shale host rock, B) Well developed sphalerite crystal, galena, and bitumen, C) Quartz and pyrite as fracture filling near major thrust fault in shale host rock, D) Vuggy filling of sparry dolomite in dolostone, E) Fault breccia cemented by white sparry dolomite, F) Selective replacement of Sphalerite in dolostone, G) Bitumen filling the joint dotted by well-developed sphalerite crystal, H) Open space filling texture of quartz-galena-sphalerite veinlet in shale host rock, I) Late galena within pyrite in dolostone, J) Sphalerite intersected by galena associated with hydrothermal dolomite, K) Late galena surrounded by brecciated sphalerite, L) Sharp zoning in sphalerite surrounded by pyrite. Abbreviations: Spdol, sparry dolomite; Qz, quartz; Sp, sphalerite; Gn, galena; Py, pyrite, (Whitney and Evans, 2010).

°C (average 208.3 °C, n=81) in hydrothermal dolomite (Table. 1, Figure 7A and C). These T_h values represent a minimum temperature of trapping of the hydrothermal fluid in the inclusion. The precise pressure during mineralization is unknown in the area. On the other hand, no boiling phenomena are seen in the fluid inclusions; according to the data of Hass (1971) this would indicate that if a hydrostatic head is assumed, then the temperature of mineralization could not have been more than about

330 °C. Thus the T_h values are probably quite close to the true (“trapping”) temperatures, and only a minimal temperature correction would be necessary. The microthermometric data of sphalerite and hydrothermal dolomite indicates that their crystallization temperatures have been mostly similar. Sphalerite, galena and hydrothermal dolomite show a close relationship with another. The results of microthermometric measurements confirm that the Irankuh mining district can be classified

Table 1. Microthermometric data of primary fluid inclusions of the Irankuh mining district.

Sample No.	Deposit	Host mineral	Number	Size (µm)	T _h (°C)	T _{m,ice} (°C)	Salinity (NaCl wt% equiv.)
40304 (surface)	Blind	Sphalerite	15	5 to 9	220 to 248	-15.4 to -16.6	19.1 to 20
40303 (surface)		Sphalerite	14	6 to 11	198 to 257	-15.2 to -16	18.8 to 19.5
40302 (surface)		Sphalerite	12	6 to 12	238 to 259	-16.7 to -17.3	20 to 20.5
40301 (surface)		Sphalerite	15	5 to 7	210 to 242	-	-
62161 (surface)	Tapeh Sorkh	Sphalerite	12	5 to 11	236 to 250	-11.6 to -12.1	15.6 to 16.1
		Dolomite	16	7 to 12	188 to 218	-10.2 to -11.2	14.2 to 15.2
62159 (surface)		Dolomite	12	5 to 8	213 to 228	-	-
62160 (surface)		Sphalerite	14	5 to 7	210 to 238	-	-
		Dolomite	11	5 to 10	212 to 223	-12 to -12.9	16 to 16.7
42106 (surface)		Sphalerite	14	8 to 14	253 to 268	-7.6 to -8.9	11.2 to 12.7
		Dolomite	7	7 to 10	208 to 214	-7.8 to -8.7	11.5 to 12.5
42316 (tunnel)		Gushfil	Sphalerite	17	5 to 12	230 to 255	-8.5 to -9.1
42313 (tunnel)	Sphalerite		16	6 to 12	255 to 271	-13 to -13.7	16.9 to 17.5
62157 (tunnel)	Sphalerite		15	7 to 12	193 to 217	-12.9 to -13.7	16.8 to 17.5
62124-1 (drill hole)	Sphalerite		13	7 to 11	255 to 275	-12.8 to -13.8	16.8 to 17.3
62124-2 (drill hole)	Sphalerite		16	5 to 8	239 to 267	-	-
	Sphalerite		14	7 to 14	260 to 280	-13.1 to -13.6	17 to 17.4
62118 (tunnel)	Dolomite		11	7 to 12	195 to 210	-11 to -11.7	15 to 15.7
	Sphalerite		12	8 to 12	245 to 256	-16.2 to -16.9	19.6 to 20.2
62137 (drill hole)	Sphalerite		14	5 to 10	240 to 270	-11.9 to -12.6	15.9 to 16.5
62154 (tunnel)	Sphalerite		14	5 to 10	240 to 270	-11.9 to -12.6	15.9 to 16.5
62163 (surface)	Romarmar five zone	Sphalerite	13	7 to 13	263 to 275	-13.2 to -13.9	17.1 to 17.7
		Dolomite	13	7 to 13	200 to 219	-10 to -10.7	13.9 to 14.7
62134 (surface)		Sphalerite	14	8 to 12	240 to 264	-4.7 to -5.9	7.5 to 9.1
62131 (tunnel)		Dolomite	11	5 to 7	190 to 205	-	-
62132 (tunnel)		Sphalerite	15	7 to 13	236 to 257	-15.9 to -17.7	19.4 to 20.8

T_h, homogenization temperature; T_m, temperature for final ice melting.

as a medium- to low-temperature deposit.

The first melting temperatures (T_{fm}) values of primary inclusions in both sphalerite and dolomite crystals cluster between -50.7 and -44.8 °C (average -47.6 °C, n=237). Comparison of the values to the eutectic temperatures of various water-salt systems (Shepherd et al., 1985; Gokce, 2000) suggests that they indicate hydrothermal fluids containing salts of CaCl₂, NaCl, KCl, and probably MgCl₂. The T_{fm} temperature fluctuations are probably due to the presence of salts such as MgCl₂. The hydrothermal dolomite alteration of host rocks indicates the presence of Mg in the ore-forming fluids. No important difference

between samples collected from surface, drill holes, and tunnels was detected; this indicates that the salt composition of the fluid was homogenous during mineralization. These salt types and compositions may be from source region of ore-fluid and/or a result of circulation of the mineralizing fluid through various sedimentary rocks.

The final ice melting temperatures (T_{m,ice}) values range from -4.7 to -17.3 °C (average -13.03 °C, n=192) in sphalerite and -7.8 to -12.9 °C (average -10.6 °C, n=55) in dolomite (Table 1 and Figure 7B and E). Salinities (wt% NaCl equivalent) of ore-forming fluids can be calculated according to the relationship between final ice melting

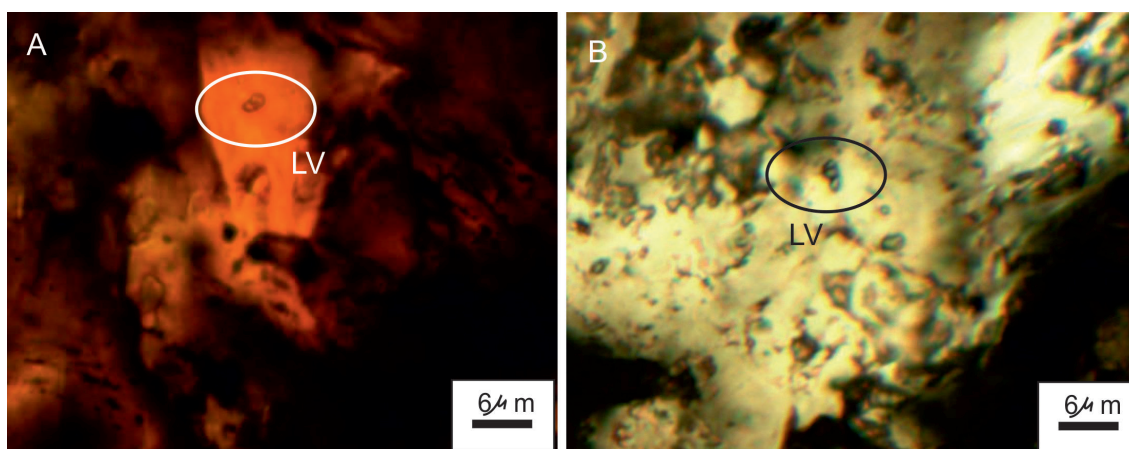


Figure 6. Photomicrographs of primary fluid inclusions in sphalerite and dolomite in the Irankuh mining district. A. Liquid-vapor inclusions in sphalerite and B. liquid-vapor inclusions in the dolomite.

temperatures and salinities (Hall and Sterner, 1988). The salinities of the hydrothermal fluids were calculated using the Microsoft Excel spreadsheet HOKIEFLINCS-H₂O-NACL (Steele-MacInnis et al., 2012; Lecumberri-Sanchez et al., 2012), and yielded wt% NaCl equivalents as follows: 7.5 to 20.5 wt% NaCl equivalent (average 16.7 wt% NaCl equivalent, n=192) in sphalerite and 11.5 to 16.8 wt% NaCl equivalent (average 14.5 wt% NaCl equivalent, n=55) in dolomite (Table 1, Figure 7C and F). These salinity data demonstrate that the ore-forming fluids were medium-salinity fluids.

SULFUR ISOTOPES

The isotopic compositions of sulfur ($\delta^{34}\text{S}$ values) in sulfide minerals and/or mineralizing fluid ($\delta^{34}\text{S}_{\Sigma\text{S}}$) in the sulfide-bearing deposits enable us to better understand both possible sources of sulfur and other metallogenic elements and help to decipher the conditions of formation of sulfides in ore deposits (Ohmoto, 1972; Ohmoto and Goldhaber, 1997). A number of factors mainly control the isotopic composition of sulfur in hydrothermal minerals and include the $f\text{O}_2$ and pH values of the hydrothermal fluids, its temperature, and the isotopic composition of the sulfur in the mineralizing fluids (Ohmoto, 1972).

The $\delta^{34}\text{S}$ values of the six galena samples were -1.8‰ to -7.3‰ with an average value of -5.88‰. The $\delta^{34}\text{S}$ values of the eight sphalerite samples were -2.2‰ to -5.7‰ with an average value of -3.82‰ (Table 2). The $\delta^{34}\text{S}$ values of galena and sphalerite occupy a narrow range and were slightly depleted in ^{34}S . According to the physical and chemical conditions ($T < 300\text{ }^\circ\text{C}$, low pH and Eh) envisaged for the ore-fluids, the main sulfur species would be H₂S (Ohmoto and Rye, 1979). The predominance of sulfide at these temperatures causes sulfide mineral $\delta^{34}\text{S}$ values to be close to the original fluid $\delta^{34}\text{S}_{\text{H}_2\text{S}}$ (Ohmoto

and Rye, 1979).

The $\delta^{34}\text{S}_{\text{CDT}}$ values of H₂S in equilibrium with galena and sphalerite were estimated to be in the range of -4.8 to +0.7‰ (average -3.37‰) and -1.8 to -5.3‰ (average -3.54‰), respectively, by evaluating the $\delta^{34}\text{S}$ values of galena and sphalerite and the average temperature of the hydrothermal fluid during the galena and sphalerite mineralization episode as 198 to 273 °C (determined by homogenization temperature measurements during fluid inclusion studies in the sphalerite or/and hydrothermal dolomite samples as closely relationship with galena and sphalerite), using the equation suggested by Li and Liu (2006) (Table 2) (Figure 8).

LEAD ISOTOPE

Pb isotopes are effective geochemical radioisotopes for understanding ore genesis and for the exploration of mineral deposits demonstrating the crustal evolution (Gulson, 1986; Lu et al., 2000). They are especially useful in assessing the source of metals, providing main information about the nature of Pb reservoir(s), constraining the timing of Pb removal from its source, and defining a geotectonic environment for ore deposits (Garipey and Dupre, 1991). Galena (PbS) is the most appropriate mineral for analysis of Pb isotope ratios within Zn-Pb deposits because it is basically free of U and is characterized by an abundant Pb content (~87 wt%); this combination guarantees that its

Pb isotopic composition remains fixed throughout the geologic time.

The results of the Pb-isotope analyses for the six galena samples (from Gushfil, Blind and Romarmar deposits) provided in Table 3. Also, two analyses of Kolah Darvazeh and Tapeh Sorkh deposits were obtained by Mirnejad et al. (2011) are added. The $^{206}\text{Pb}/^{204}\text{Pb}$, $^{207}\text{Pb}/^{204}\text{Pb}$, and

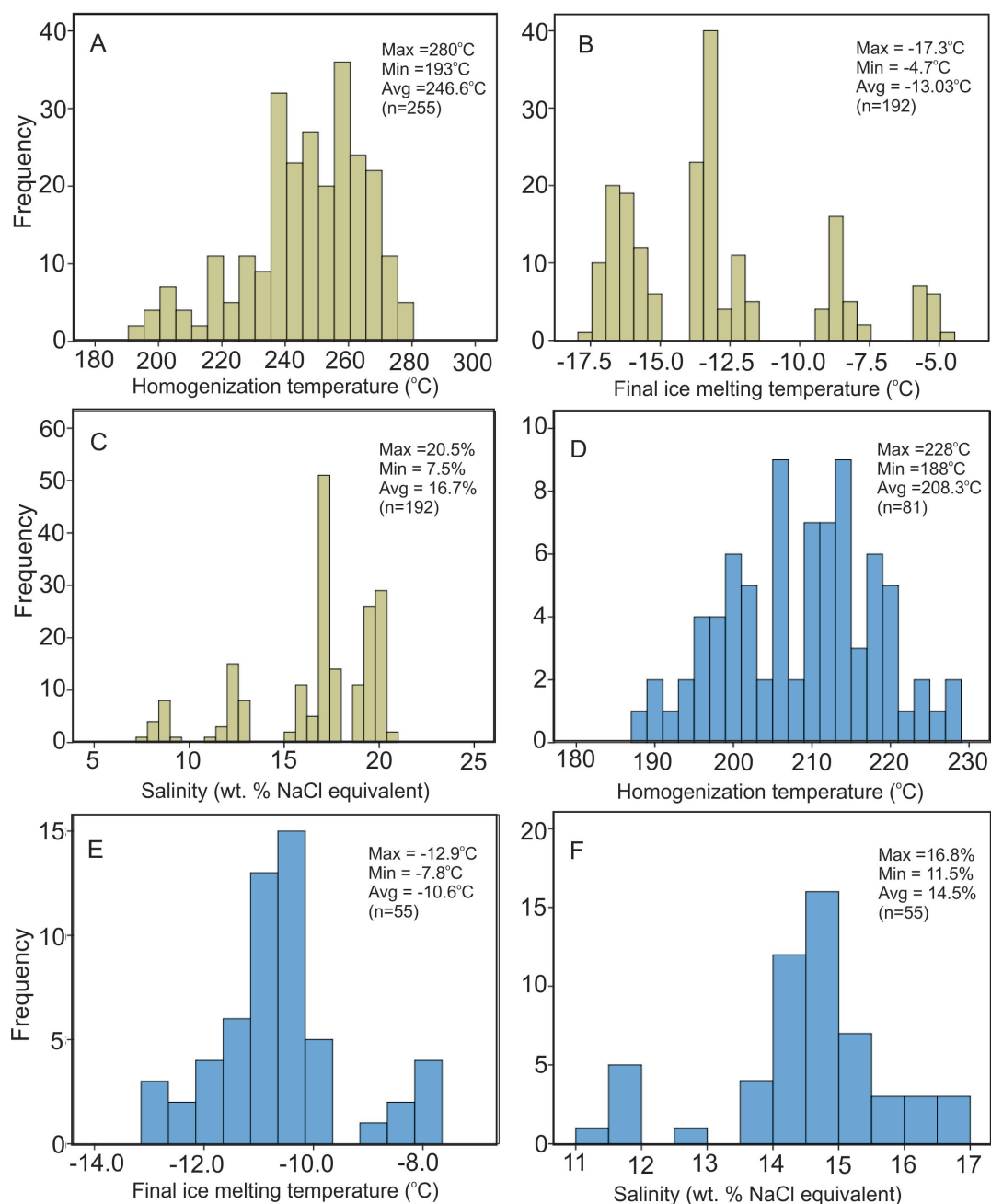


Figure 7. Histogram showing the thermodynamic data of primary fluid inclusions in the Irankuh mining district. A. Homogenization temperature (°C) histogram in sphalerite, B. final ice melting temperature (°C) histogram in sphalerite, C. salinity (wt% NaCl equivalent) histogram in sphalerite, D. Homogenization temperature (°C) histogram in dolomite, E. final ice melting temperature (°C) histogram in dolomite, and F. salinity (wt% NaCl equivalent) histogram in dolomite.

$^{208}\text{Pb}/^{204}\text{Pb}$ ratios of the samples span narrow ranges of 18.419-18.476 (average of 18.456), 15.634-15.663 (average of 15.656), and 38.562-38.670 (average of 38.642), respectively.

Pb isotope research is principally used to confine the probable source rocks of the metals in deposits. When the

isotope data are plotted on Stacey and Kramers' (1975) model curves for average crustal Pb isotope evolution, the $^{207}\text{Pb}/^{204}\text{Pb}$ and $^{208}\text{Pb}/^{204}\text{Pb}$ ratios plot above the evolution curves and clearly show a crustal source (Figure 9A and B). Possible Pb sources also have been checked using the plumbotectonic diagrams of Zartman and Haines (1988)

Table 2. Sulfur isotope compositions of the Irankuh mining district.

Sample No.	Deposit	Mineral	$\delta^{34}\text{S}_{\text{sulfide}}$ (‰)CDT	Average T_h (°C) (fluid calculated)	1000 $\ln\alpha$ (Li and Liu, 2006)	$\delta^{34}\text{S}_{\text{H}_2\text{S}}$ (‰)
40304 (surface)	Blind	Galena	-1.8	237	-2.5	+0.7
62137 (drill hole)	Gushfil	Galena	-6.3	251	-2.3	-4.0
62129 (tunnel)	Romarmar five zone	Galena	-6.8	236	-2.5	-4.3
62131 (tunnel)		Galena	-6.9	198	-2.9	-4.0
62132 (tunnel)		Galena	-6.2	247	-2.4	-3.8
62146 (tunnel)		Galena	-7.3	236	-2.5	-4.8
40302 (surface)	Blind	Sphalerite	-3.1	248	+0.4	-3.5
42106 (surface)	Tapeh Sorkh	Sphalerite	-3.2	244	+0.4	-2.8
62148 (surface)		Sphalerite	-3.1	244	+0.4	-2.7
62118 (tunnel)	Gushfil	Sphalerite	-3.2	273	+0.3	-2.9
62124 (tunnel)		Sphalerite	-2.2	250	+0.4	-1.8
62137 (drill hole)		Sphalerite	-5.7	250	+0.4	-5.3
62134 (surface)	Romarmar five zone	Sphalerite	-5.2	252	+0.4	-4.8
62147 (surface)		Sphalerite	-4.9	255	+0.4	-4.5

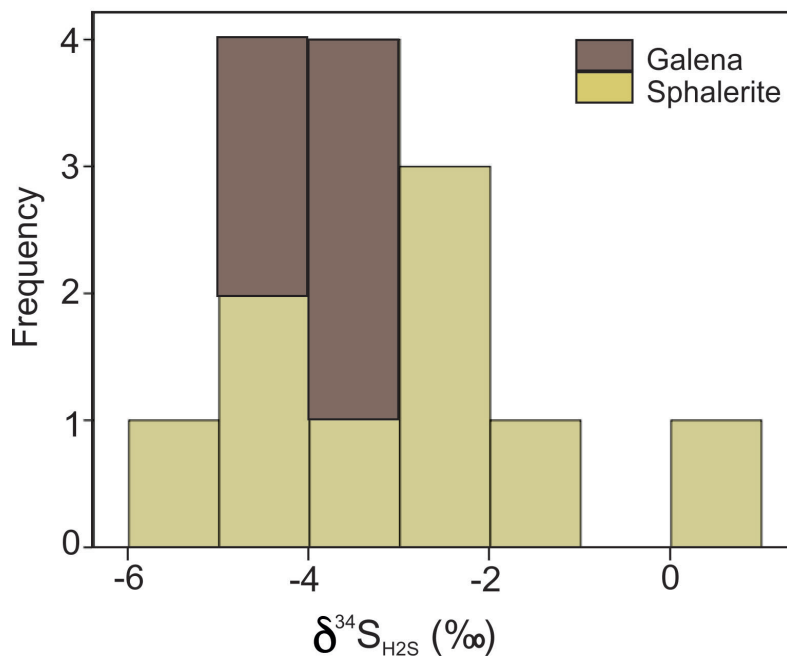


Figure 8. Histogram of $\delta^{34}\text{S}_{\text{H}_2\text{S}}$ in equilibrium with galena and sphalerite at a calculated temperatures (based on the average temperature of the hydrothermal fluid during the galena and sphalerite mineralization period as 198-273 °C, using the Li and Liu (2006) equation).

(Figure 10A). In Figure 9A, the $^{207}\text{Pb}/^{204}\text{Pb}$ vs $^{206}\text{Pb}/^{204}\text{Pb}$ data cover an area below the Upper Crust curve, suggesting a homogen source for the Pb. In the $^{208}\text{Pb}/^{204}\text{Pb}$ vs $^{206}\text{Pb}/^{204}\text{Pb}$ diagram (Figure 9B), all samples plot above the upper crust, mantle, and orogen average values, showing a major contribution of Th-derived lead.

DISCUSSION

Evolution of ore-forming fluids

The results of fluid inclusion analyses from the Irankuh Pb-Zn mining district revealed that the ore-forming fluids were low- to medium-temperature, medium-salinity H_2O -NaCl system fluids. The pressure-temperature diagram

Table 3. Lead-isotope composition of the analyzed samples in the Irankuh mining district. Kolah Darvazeh and Tapeh Sorkh samples from Mirnejad et al. (2011).

Sample	Deposit	²⁰⁶ Pb/ ²⁰⁴ Pb	²⁰⁷ Pb/ ²⁰⁴ Pb	²⁰⁸ Pb/ ²⁰⁴ Pb
40304-1 (surface)	Blind	18.461	15.660	38.662
62137-1 (drill hole)	Gushfil	18.476	15.658	38.670
62153-1 (drill hole)	Romarmar two zone	18.457	15.660	38.657
62146-1 (tunnel)	Romarmar five zone	18.461	15.660	38.653
62131-1 (tunnel)		18.463	15.663	38.653
62132-1 (tunnel)		18.464	15.663	38.655
1 (surface)	Kolah Darvazeh	18.419	15.634	38.562
2 (surface)	Tapeh Sorkh	18.450	15.651	38.627

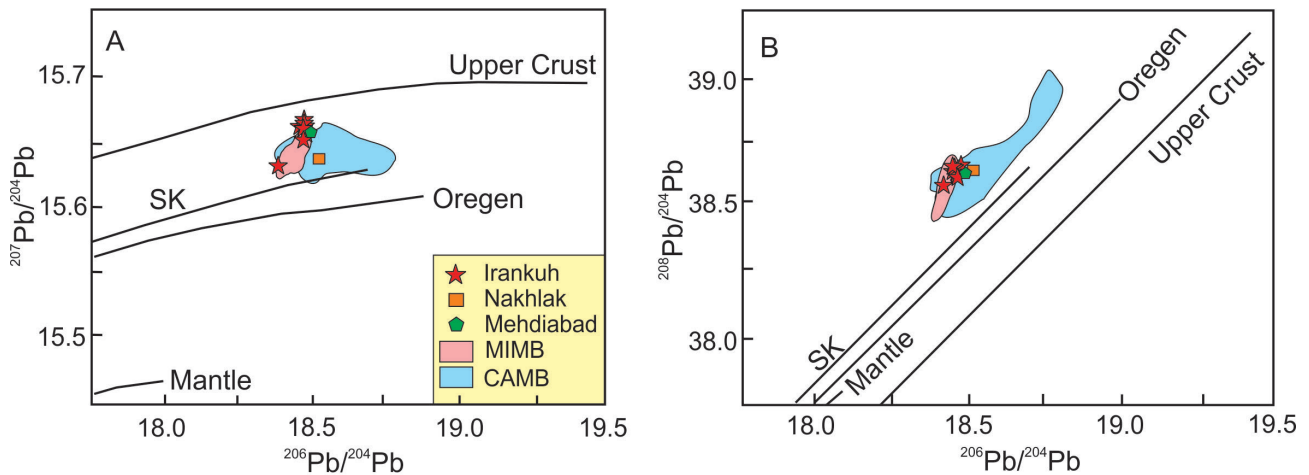


Figure 9. Pb isotope ratios of galena samples in the Irankuh mining district comparison with Naxhlak, Mehdiabad, Malayer-Isfahan Metallogenic belt (MIMB) and Central Alborz Metallogenic belt (CAMB) MVT-type deposits on a ‘plumbotectonic’ diagram (Zartman and Doe, 1981) and Stacey and Kramers (1975) (SK) curve.

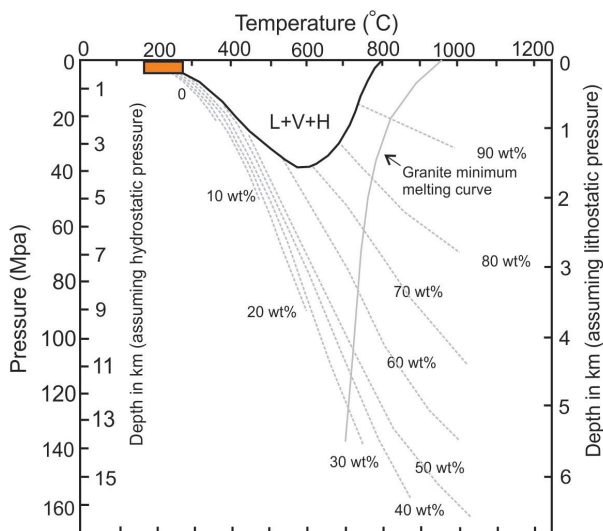


Figure 10. Pressure-Temperature diagram showing phase relationships in the NaCl-H₂O system at lithostatic and hydrostatic pressures (Fournier, 1999). L= liquid, V= vapor, H= halite. Thin dashed lines are contours of constant wt. percent NaCl dissolved in brine. Filled gray line indicates granite minimum melting curve. Filled dark line shows the three-phase boundary, L+V+H, for the system NaCl-KCl-H₂O with Na/K in solution fixed by equilibration with albite and K-feldspar at the indicated temperatures. Location of Irankuh fluid inclusions plotted on it.

of Fournier (1999) indicates that the pressure during formation of the Irankuh deposits was approximately <10 MPa, which is equivalent to a depth of approximately <1 km, assuming hydrostatic and lithostatic pressure (Figure 10). Therefore, the veins were formed at shallow depth, as confirmed by the structure and texture of the ore minerals. The salinity vs homogenization temperature diagram (Figure 11), used for possible trends of fluid evolution, not shows positive or negative correlations, which implies to fluid mixing and fluid boiling, respectively (Shepherd et al., 1985). On the fluid evolution diagram (Figure 11A and B), Irankuh fluid inclusion samples are similar to trend 5 represents cooling of fluid for both sphalerite and hydrothermal dolomite. It seems clear for the Irankuh deposits that cooling played an important role in formation of ore veins. However, the role of organic materials and the reduced environment should also be considered.

Salinity changes indicate that fluids with different salinity played a role in the formation of both sphalerite and dolomite minerals. Four types of sphalerite and two types of dolomite with different salinity can be distinguished (Figure 11A and B). Some sphalerites are made up of a fluid with a salinity of more than 18 wt% NaCl equivalent, which is seen in Blind, Gushfil, and Romarmar deposits. The salinity of fluid that form most of the sphalerites in Gushfil and less in the Romarmar and Tapeh Sorkh deposits is between 15 to 18 wt% NaCl equivalent. Sphalerite samples with salinity of between 11 to 13 wt% NaCl equivalent are seen in the Gushfil and Tapeh Sorkh deposits, whereas sphalerites with a salinity of less than 9 wt% NaCl equivalent are found only in the Romarmar deposit (Figure 11A). Also, dolomite samples are made up of two different fluids with a salinity of 13 to 17 wt% NaCl equivalent and less than 13 wt% NaCl equivalent that low salinity dolomites found only in the Tapeh Sorkh deposit (Figure 11B). There are no significant mineralogical differences between sphalerite and dolomite samples with different salinity. Increase of salinity can be attributed to the mixing of the initial ore-resolution and the basal brines with the same temperature during the upward migration of the fluid. Basinal hydrothermal systems involve connate water, water from diagenetic reactions, and meteoric recharge (Kharaka and Hanor, 2007); these types of fluids produce MVT deposits (Leach and Sangster, 1993). According to Kesler et al. (1995), MVT fluids have salinities of 10 to 30 wt%, which result from evaporation and dissolution of evaporates.

Sulfur and metal sources

The relatively narrow range in $\delta^{34}\text{S}$ values displayed by sulfur-bearing minerals (galena and sphalerite) indicates a uniform isotopic composition of the source and/or uniform conditions governing the isotopic fractionation

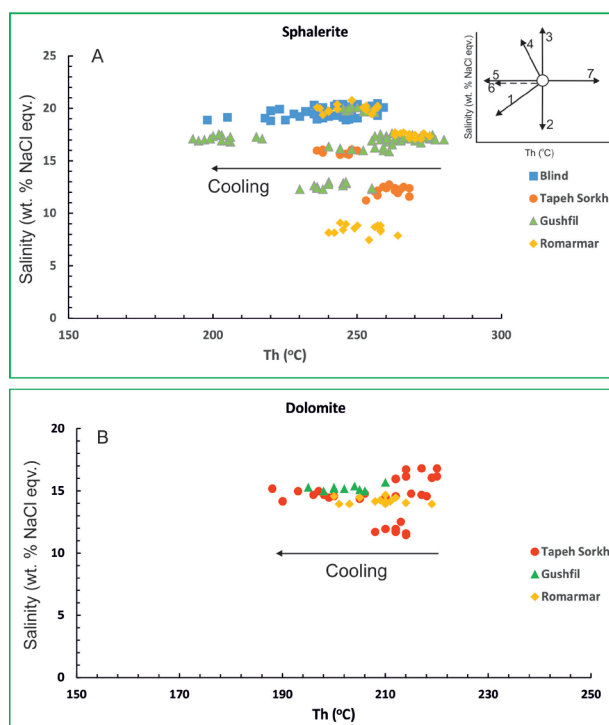


Figure 11. Homogenization temperature versus salinity of fluid inclusions in the Irankuh mining district. A. Sphalerite and B. Dolomite. Several possible trends of fluid evolution in a temperature-salinity diagram from Shepherd et al. (1985). Trend 1 represents primitive fluid A mixed with cold and low salinity fluid B, trends 2 and 3 represent the result of fluid A isothermally mixing with different salinity fluid B, trend 4 represents the salinity of residual phase increased, caused by boiling of fluid A, trend 5 represents cooling of fluid A, trend 6 represents necking of the fluid inclusion, trend 7 represents leakage of fluid inclusions during heating.

between sulfur species in the ore-forming fluids during mineralization. In Mississippi Valley-type environments, seawater sulfates of crustal origin were a source of sulfide sulfur; nevertheless, individual districts may exhibit a complex and distinct mode of sulfur derivation (White, 2013). The sulfur isotope data of other Mississippi Valley-type deposits indicate two major populations, one centered between -5‰ and +15‰ and one greater than +20‰ (Seal, 2006). The sulfur isotope values of galena and sphalerite from the Irankuh mining district overlap the first population of sulfide sulfur isotopes of MVT deposits. The negative $\delta^{34}\text{S}$ values are specifically similar to Pb-rich Southeast Missouri-type MVT deposits (Figure 13). Also, comparison of $\delta^{34}\text{S}$ values from Irankuh with Ahangaran and Emarat (MIMB, Figure 1) and Nakhllak (YAMB, Figure 1) MVT deposits (Figure 13) show more negative contents in the study area. These deposits (Ahangaran, Emarat, and Nakhllak) mostly overlap the

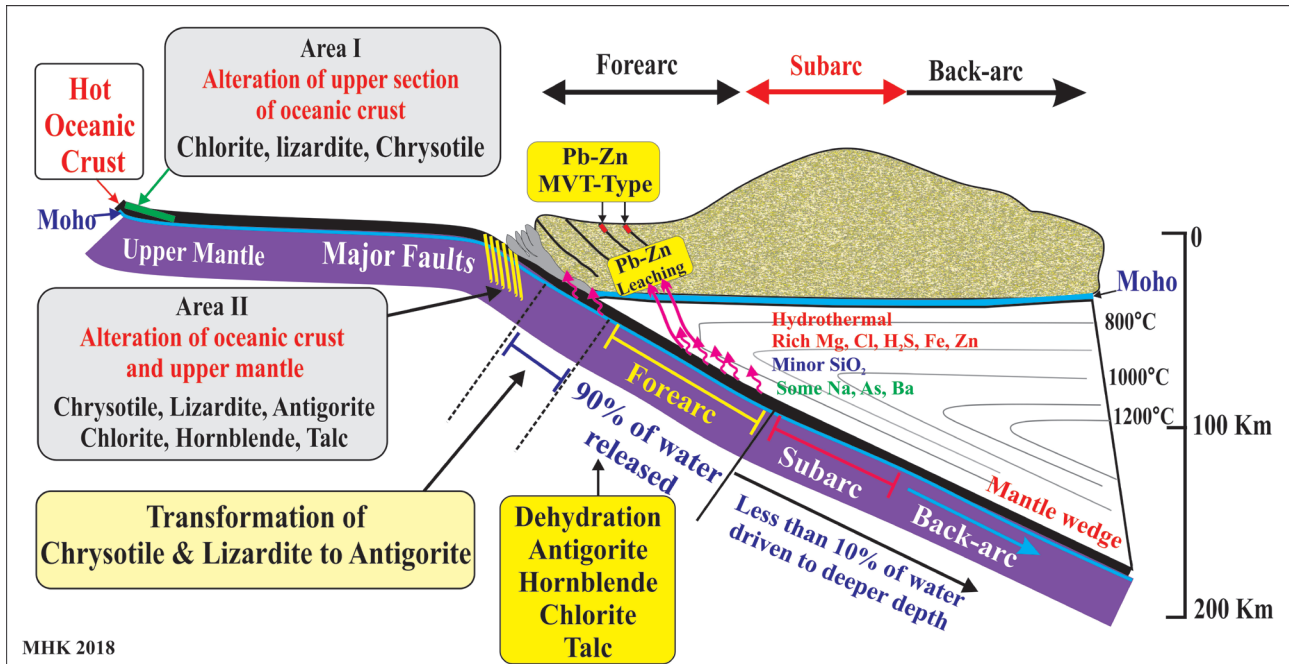


Figure 12. A Hot oceanic slab, dehydrates and releases most of the water within the forearc region (Modified after Karimpour and Sadeghi, 2018).

Upper Mississippi Valley deposits. Although, the negative $\delta^{34}\text{S}$ values of galena from Ahangaran deposit have reported similar to galena samples of Irankuh (Akbari, 2017; Figure 13). Based on new hypothesis for formation of Irankuh deposits (Karimpour and Sadeghi, 2018), the hydrothermal fluid originated from the dehydration of an oceanic subduction slab is changed in during the upward migration to shallow depths and then the values of S isotope cannot show a particular source for sulfur. The lack of relationship with igneous activity in the study area indicates a magmatic source of sulfur is excluded. However, the negative $\delta^{34}\text{S}$ values are similar to the values of typical magmatic sulfur ($0\text{‰}\pm 5\text{‰}$, Ohmoto and Goldhaber, 1997). Consistently, the salinity contents of fluid inclusions argue against a magmatic source for fluids. A possible source for ^{34}S -depleted sulfur would be sulfide-bearing sedimentary rocks. In fact, the use of stable isotopes to determine the origin of ore-fluid and the type of mineralization is not appropriate. Field evidence and petrographic, mineralogical and geochemical studies can determine the origin, conditions and relative time of formation of deposit.

The Pb isotope values of Irankuh samples are similar to other famous MVT deposits of Iran (such as Nakhlak and Mehdiabad) and the same mineralization in MIMB and CAMB (Figure 9). Zartman and Doe (1981) proposed a mixed source (continental crust and mantle) for Pb when the amount of Pb isotopic data plots between the ‘upper

crust’ and ‘orogen’ growth curves (Figure 9A). Karimpour and Sadeghi (2018) suggested Pb isotopic compositions of MIMB Pb-Zn deposits are $^{206}\text{Pb}/^{204}\text{Pb}$ from 18.42 to 18.45; $^{208}\text{Pb}/^{204}\text{Pb}$ from 38.53 to 38.62 and $^{207}\text{Pb}/^{204}\text{Pb}$ from 15.63 to 15.65. Very low radiogenic Pb isotopes indicate that Pb-isotopes had an oceanic slab source and were slightly contaminated by the basement rocks. Pb isotopic compositions of MIMB Pb-Zn deposits are similar to some of the Central Appalachian Pb-Zn MVT-type deposits (Heyl et al., 1966; Kesler et al., 1994).

Genetic model

The Irankuh mining district has many geological features that are comparable to MVT Zn-Pb deposits (Sangster, 1990; Leach et al., 2005). Most previous studies emphasized on the MVT type of mineralization based on geology, alteration, mineralization, geochemistry, and fluid inclusion studies, which is carried out in parts of the mining district or in one of its deposits (Rastad, 1981; Ghazban et al., 1994; Ghasemi, 1995; Reichert, 2007; Hosseini-Dinani et al., 2015; Hosseini-Dinani and Aftabi, 2016; Karimpour et al., 2018; Karimpour and Sadeghi, 2018; Saboori et al., 2019; Karimpour et al., 2019). The most important similarities between the Irankuh and MVT Zn-Pb deposits are type of host rock, epigenetic and stratabound form, no relationship with igneous activity, ore controls, wall-rock alteration style, structure, texture characteristics of the orebody, mineral composition, and

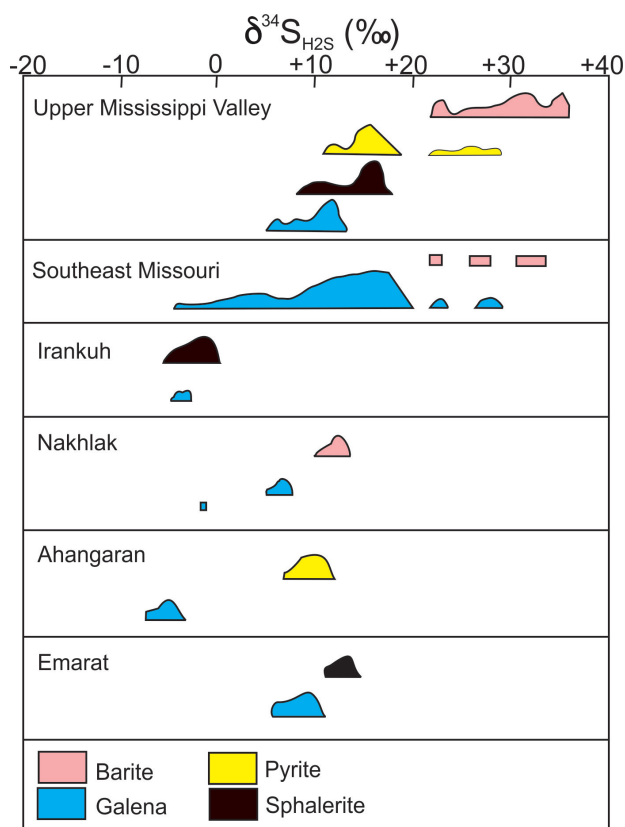


Figure 13. The $\delta^{34}\text{S}$ values in the two main groups of Mississippi Valley-type Pb-Zn deposits (after Ohmoto and Rye, 1979) compared to $\delta^{34}\text{S}$ values of galena and sphalerite from the Irankuh mining district. The $\delta^{34}\text{S}$ values of Ahangaran from Akbari (2017), Emarat from Ehya et al. (2010), and Nakhlak from Jazi et al. (2017). The location of three deposits is shown on Figure 1.

nature of ore-forming fluids (Mg-rich, low- to medium-temperature and medium salinity).

Karimpour and Sadeghi (2018) suggested new hypothesis for formation of MIMB Pb-Zn MVT deposits that Irankuh district is a part of this belt. They believed that these deposits were occurred in forearc tectonic setting. More than 90% of all the water within the oceanic slab was released in the depth zone of the forearc region (depth of 30 to 50 km). The hydrothermal fluid originated from the dehydration of Neo-Tethys oceanic subduction slab (hot slab), which liberated Pb, Zn, and other metals, and may have removed metals from rocks and organic material of the continental crust. Deep-seated thrust faults formed during the early stages of subduction and played an important role in the upward migration of hydrothermal fluids from the basement to shallow depths (Karimpour and Sadeghi, 2018) (Figure 12). Additionally, Karimpour et al. (2019) suggested the MVT deposits of MIMB were

predominantly formed in an age range of 66 to 56 million years ago (Palaeocene) based on geological features. This claim is confirmed by Re-Os pyrite dating. The geochronology of pyrite in Irankuh district based on Re-Os method indicate age of Irankuh Pb-Zn mineralization is 66.5 ± 1.6 Ma (Liu et al., 2019).

The formation of Irankuh deposits can be summarized in Figure 14. The hydrothermal fluid originated from the dehydration of an oceanic subduction slab (forearc area), which is MgO-rich and low SiO_2 , was migrated to shallow depths. H_2O , SO_4 , Cl, Zn±Ba and other elements were released from the plate during subduction. The water release temperature from the oceanic slab at a depth of 40 km is about 300 °C. By passing through in regions with high thermal gradient, the temperature rises to over 300 °C. The temperature decreases to less than 300 °C with upwards migration of ore-fluid to shallow depth and decreasing of thermal gradient. This ore-fluid causes metasomatism on the mantle wedge, richen in Mg, Fe, and other elements and entered the continental crust basement. The reaction takes place between the hydrothermal solution and the continental crust and some elements such as Pb, Zn and Ba can be dissolved by leaching and reaction. The final hydrothermal fluid rises to shallow depths by deep-seated thrust faults (Figure 14). The

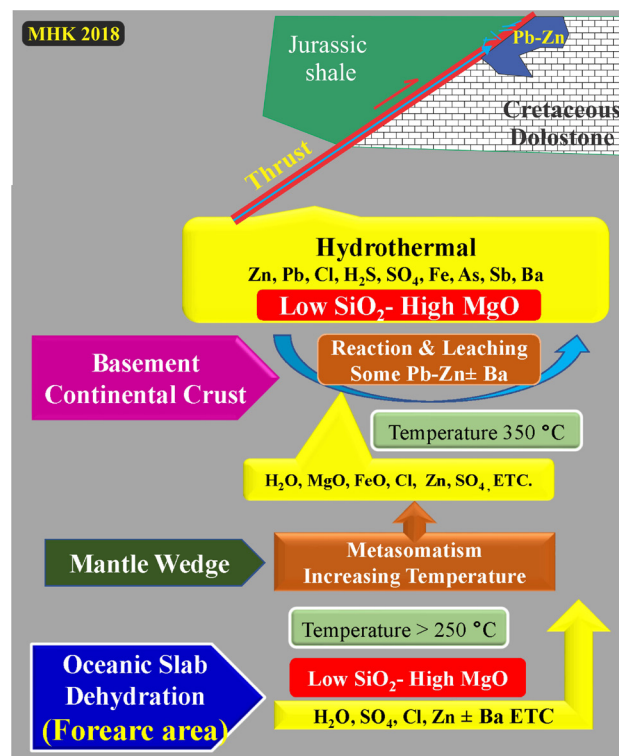


Figure 14. Schematic and simplified plan of formation of Irankuh mining district.

ore-fluid, in appropriate temperature and pH conditions, has deposited its metals on the Cretaceous dolostone or Jurassic shale, where the paragenesis, alteration, shape, and dimension of mineralization are completely different in the two host rocks.

CONCLUSIONS

(1) Hydrothermal fluid migrated from the dehydrated subducted plate to the locations of the orebodies, moving upward along branches of the thrust faults to the Cretaceous dolostone and Jurassic shale. The thrust faults were very important for the formation Irankuh Pb-Zn deposits. The strike-slip faults is considered as destructive types, because they displaced the mineralization. Mineralization mostly occurs within dolostone units where it is principally deposited as replacements of dolostone; with some open space filling in tectonic and solution breccia. Minor mineralization occurs in Jurassic shale as stockwork veinlets. Mineralization also filled fractures and joints near major thrust faults. The alteration zone is marked by an assemblage of dolomite, Fe-rich dolomite, ankerite, and quartz. The Fe-rich dolomite and ankerite are seen within dolostone host rock, whereas low Fe-dolomite and quartz mostly occur in Jurassic shale. The ore vein includes sphalerite, galena, and bitumen associated with minor pyrite and barite in dolostone and sphalerite, galena, pyrite, and bitumen associated with minor chalcopyrite in shale. Therefore, the paragenesis, alteration, shape, and dimension of mineralization are completely different in the two host rocks.

(2) Fluid inclusion data revealed that the ore-forming fluids included significant amounts of divalent cations (CaCl_2 , KCl , and MgCl_2) along with NaCl . Microthermometric studies and composition measurements of fluid inclusions indicated that the general characteristics of the ore-forming fluids involved medium- to low-temperature and medium-salinity in the $\text{NaCl-H}_2\text{O}$ system. The relation of homogenization temperature and fluid salinity, combined with the ore deposit geology, provide proof that cooling was the main process in the evolution of the ore-forming fluids. However, the role of organic materials should also be considered. Based on microthermometric data, four types of sphalerites and two types of hydrothermal dolomites with the same temperatures and different salinity were recognized. The basinal brines may play a role in increasing salinity.

(3) The values of $\delta^{34}\text{S}$ in galena and sphalerite samples from the Irankuh deposits ranged between -1.8‰ and -7.3‰ . The $\delta^{34}\text{S}_{\text{H}_2\text{S}}$ values in equilibrium with galena and sphalerite were calculated to be in the range of -1.8 to $+0.7\text{‰}$ (average -3.4‰). The possible source of sulfur may be sulfide-bearing sedimentary rocks. But the S isotope values cannot show a particular source because

many changes during the upward migration of ore-fluid.

(4) The Pb isotopes suggest that the source of the lead was from the subducted basaltic oceanic crust, contaminated with lead from the continental crust. This may have been from sediment eroded from the continental on to the seafloor, where it was incorporated into the subducted plate.

In conclusion, the geological, structural, alteration, and mineralization information combined with fluid inclusion and isotope geochemistry data suggest that a hydrothermal fluid originated from the dehydration of Neo-Tethys oceanic subduction slab (forearc area), which is MgO-rich and low SiO_2 , ascending upward through thrust faults that cut up through the stratigraphy. Some elements were released from the plate during subduction and some metals were leached from the continental crust basement. Finally, we strongly suggest that Irankuh mining district is a typical MVT ore deposit in Iran.

ACKNOWLEDGEMENTS

This study was supported by a grant from Research Foundation of Ferdowsi University of Mashhad (Iran) (Project No. 40221.3, date: 3 March 2016). We thank Bama Company especially Mr. Eslami, Naghshineh, Roshan and Dr. Mohammadkhani for all financial and spiritual assistance.

REFERENCES

- Agard P., Omrani J., Jolivet L., Mouthereau F., 2005. Convergence history across Zagros, Iran: Constraints from collisional and earlier deformation. *International Journal of Earth Sciences* 94, 401-419.
- Akbari Z., 2017. Model for the genesis of Ahangaran Fe-Pb deposit (SE of Malayer), based on ore types, geochemistry and stable isotopic studies. Unpublished Ph.D. thesis, Tehran, Tarbiat Modares University.
- Anderson G.M., 1983. Some geochemical aspects of sulfide precipitation in carbonate rocks. In: *International Conference on Mississippi Valley Type Lead-Zinc Deposits (Eds.): G. Kisvarsanyi, S.K. Grant, W.P. Pratt and J.W. Keonig, University of Missouri, Rolla, Missouri, 61-76.*
- Alavi M., 2004. Regional stratigraphy of the Zagros fold-thrust belt of Iran and its proforeland evolution. *American journal of science*, 304, 1-20.
- Appold M.S. and Garven G., 1999. The hydrology of ore formation in the Southeast Missouri District: numerical models of topography-driven fluid flow during the Ouachita Orogeny. *Economic Geology* 94, 913-936.
- Arvin M., Pan Y., Dargahi S., Malekizadeh A., Babaei A., 2007. Petrochemistry of the Siah-Kouh granitoid stock southwest of Kerman, Iran: Implications for initiation of Neotethys subduction. *Journal of Asian Earth Sciences* 30, 474-489.
- Bodnar R.J., 2003. Introduction to fluid inclusions. In: *Fluid Inclusions: Analysis and Interpretation (Eds.): I. Samson,*

- A. Anderson, D. Marshall, Mineral. Assoc. Canada, Short Course 32, 1-8.
- Berberian M. and King, G., 1981. Towards a paleogeography and tectonic evolution of Iran. *Canadian Journal of Earth Sciences* 18, 210-265.
- Boveiri-Konari M., Rastad E., Peter J.M., 2017. A sub-seafloor hydrothermal syn-sedimentary to early diagenetic origin for the Gushfil Zn-Pb-(Ag-Ba) deposit, south Esfahan, Iran. *Neues Jahrbuch für Mineralogie-Abhandlungen* 194, 61-90.
- Ehya F., Lotfi M., Rasa I., 2010. Emarat carbonate-hosted Zn-Pb deposit, Markazi Province, Iran: A geological, mineralogical and isotopic (S, Pb) study. *Journal of Asian Earth Science* 37, 186-194.
- Fournier R.O., 1999. Hydrothermal processes related to movement of fluid from plastic into brittle rock in the magmatic-epithermal environment. *Economic Geology* 94, 1193-1212.
- Garipey C. and Dupre B., 1991. Pb isotopes and crust-mantle evolution. In: *Application of Radiogenic Isotope-systems to Problems in Geology* (Eds.): L. Heaman and J.N. Ludden, Short Course Handbook Mineralogical Association of Canada, Toronto, 191-224.
- Garven G., 1985. The role of regional fluid flow in the genesis of the Pine Point deposit, Western Canada Sedimentary Basin. *Economic Geology* 80, 307-324.
- Ge S. and Garven G., 1992. Hydromechanical modeling of tectonically driven groundwater flow with application to the Arkoma Foreland Basin. *Journal of Geophysical Research* 97 (B6), 9119-9144.
- Ghasemi A., 1995. Facies analysis and geochemistry of Kolah-Darvazaeh, Goud-Zendan, and Khaneh-Gorgi Pb-Zn deposits from south of Irankuh. M.Sc. thesis, Tarbiat Modares University, Tehran, Iran, 158 pp. (in Persian).
- Ghasemi A. and Talbot C.J., 2005. A new tectonic scenario for the Sanandaj-Sirjan Zone (Iran). *Journal of Asian Earth Sciences* 26, 683-693.
- Ghazban F., McNutt R.H., Schwarcz H.P., 1994. Genesis of sediment-hosted Zn-Pb-Ba deposits in the Irankuh district, Esfahan area, west-central Iran. *Economic Geology* 89, 1262-1278.
- Ghorbani M., 2002. An introduction to economic geology of Iran. National Geosciences Database of Iran, Report.
- Gokce A., 2000. Ore deposits. Cumhuriyet University Publication 100, 1-336.
- Golonka J., 2004. Plate tectonic evolution of the southern margin of Eurasia in the Mesozoic and Cenozoic. *Tectonophysics* 381, 235-273.
- Gulson B.L., 1986. *Lead Isotopes in Mineral Exploration*. Elsevier Science Publishers, Amsterdam (Netherlands), 245 pp.
- Hall D.L. and Sterner S.M., 1988. Freezing point depression of NaCl-KCl-H₂O solution. *Economic Geology* 83, 197-202.
- Hass J.L., 1971. The effect of salinity on the maximum thermal gradient of a hydrothermal system at hydrostatic pressure. *Economic Geology* 66, 940-946.
- He L., Song Y., Chen K., Hou Z., Yu F., Yang Z., Wei J., Li Z., Liu Y., 2009. Thrust-controlled, sediment-hosted, Himalayan Zn-Pb-Cu-Ag deposits in the Lanping foreland fold belt, eastern margin of Tibetan Plateau. *Ore Geology Review* 36, 106-132.
- He X.X., Zhu X., Yang C., Tang S.H., 2005. High-precision analysis of Pb isotope ratios using MC-ICP-MS. *Acta Geoscientia Sinica* 26, 19-22.
- Hitzman M.W., Reynolds N.A., Sangster D., Allen C.R., Carman C.E., 2003. Classification, genesis, and exploration guides for nonsulfide zinc deposits. *Economic Geology* 98, 685-714.
- Horton B.K., Hassanzadeh J., Stockli D.F., Axen G.J., Gillis R.J., Guest B., Amini A., Fakhari M.D., Zamanzadeh S.M., Grove M., 2008. Detrital zircon provenance of Neoproterozoic to Cenozoic deposits in Iran: Implications for chronostratigraphy and collisional tectonics. *Tectonophysics* 451, 97-122.
- Hosseini-Dinani H. and Aftabi A., 2016. Vertical litho-geochemical halos and zoning vectors at Goushfil Zn-Pb deposit, Irankuh district, southwestern Esfahan, Iran: Implications for concealed ore exploration and genetic models. *Ore Geology Reviews* 72, 1004-1021.
- Hosseini-Dinani H., Aftabi A., Esmaili A., Rabbani M., 2015. Composite soil-geochemical halos delineating carbonate-hosted zinc-lead-barium mineralization in the Irankuh district, Esfahan, west-central Iran. *Journal of Geochemical Exploration* 156, 114-130.
- Heyl A.V., Delevaux M., Zartman R.E., Brock M.R., 1966. Isotopic study of galenas from the upper Mississippi Valley, the Illinois-Kentucky, and some Appalachian Valley mineral districts. *Economic Geology* 61, 933-961.
- Jazi M.A., Karimpour M.H., Malekzadeh Shafaroudi A., 2017. Nakhlak carbonate-hosted Pb±(Ag) deposit, Esfahan province, Iran: a geological, mineralogical, geochemical, fluid inclusion, and sulfur isotope study. *Ore Geology Reviews* 80, 27-47.
- Karimpour M.H., Malekzadeh Shafaroudi A., Esmaili Sevieri A., Shabani S., Allaz J.M., Stern C.R., 2018. Geology, mineralization, mineral chemistry, and chemistry and source of ore fluid of Irankuh Pb-Zn mining district, south of Esfahan. *Iranian Journal of Economic Geology* 9, 267-294. (In Persian with English extended abstract).
- Karimpour M.H., Malekzadeh Shafaroudi A., Alaminia Z., Esmaili Sevieri A., Stern C.R., 2019. New hypothesis on time and thermal gradient of subducted slab with emphasis on dolomitic and shale host rocks in formation of Pb-Zn deposits of Irankuh-Ahangaran belt. *Iranian Journal of Economic Geology* 10, 677-706. (In Persian with English extended abstract).
- Karimpour M.H. and Sadeghi M., 2018. Dehydration of hot oceanic slab at depth 30-50 km: KEY to formation of Irankuh-Emarat Pb-Zn MVT belt, Central Iran. *Journal of Geochemical Exploration* 194, 88-103.

- Kesler S.E., Appold M.S., Cumming G.L., Krstic D., 1994. Lead isotope geochemistry of Mississippi Valley-type mineralization in the Central Appalachians. *Economic Geology* 89, 1492-1500.
- Kesler S.E., Appold M.S., Martini A.M., Walter L.M., Huston T.J., Kyle J.R., 1995. Na-Cl-Br systematics of mineralizing brines in Mississippi Valley-type deposits. *Geology* 23, 641-644.
- Kesler S.E., Carrigan C.W., 2002. Discussion on "Mississippi Valley-type lead-zinc deposits through geological time: implications from recent age-dating research" by D.L. Leach, D. Bradley, M.T. Lewchuk, D.T.A. Symons, G. de Marsily, J. Brannon (2001) *Mineralium Deposita* 36, 711-740. *Mineralium Deposita* 37, 800-802.
- Khalaji A.A., Esmaily D., Valizadeh M.V., Rahimpour H., 2007. Petrology and geochemistry of the granitoid complex of Boroujerd, Sanandaj-Sirjan zone, western Iran. *Journal of Asian Earth Sciences* 29, 859-877.
- Kharaka Y.K. and Hanor J.S., 2007. Deep fluids in the continents: I. Sedimentary basins. In: *Surface and Ground Water. Weathering and Soils*, (Ed.) J.I. Drever, Treatise on Geochemistry 5, 1-48.
- Leach D.L. and Sangster D.F., 1993. Mississippi valley-type lead-zinc deposits. In: *Mineral Deposit Modeling*, (Eds.) R.V. Kirkham, W.D. Sinclair, R.I. Thorp, J.M. Duke, Geological Association of Canada Special Paper 40, 289-314.
- Leach D.L., Bradley D.C., Lewchuk M., Symons D.T.A., Brannon J., de Marsily G., 2001. Mississippi Valley-type lead-zinc deposits through geological time: implications from recent age-dating research. *Mineralium Deposita* 36, 711-740.
- Leach D.L., Sangster D.F., Kelley K.D., Large R.R., Garven G., Allen C.R., Gutzmer J., Walters S., 2005. Sediment-hosted lead-zinc deposits: a global perspective. *Economic Geology* 100th Anniversary Volume, 561-608.
- Leach D.L., Taylor R.D., Fey D.L., Diehl S.F., Saltus R.W., 2010. A Deposit Model for Mississippi Valley-Type Lead-Zinc Ores: Chapter A in *Mineral Deposit Models for Resource Assessment*, 2328-0328.
- Lecumberri-Sanchez P, Steel-MacInnis M, Bodnar R.J., 2012. A numerical model to estimate trapping conditions of fluid inclusions that homogenize by halite disappearance. *Geochim Cosmochim Acta* 92, 14-22.
- Li Y. and Liu J., 2006. Calculation of sulfur isotope fractionation in sulfides. *Geochimica et Cosmochimica Acta* 70, 1789-1795.
- Liu Y., Song Y., Fard M., Zhou L., Hou Z., Kendrick M.A., 2019. Pyrite Re-Os age constraints on the Irankuh Zn-Pb deposit, Iran, and regional implications. *Ore Geology Reviews* 104, 148-159.
- Lu Z.C., Duan G.Z., Liu C.Q., Hao L.B., Li D.C., Wei C.D., 2000. Daxing'anling Ag deposit types, metallogenic series and metallogenic geochemical characteristics. *Bulletin of Mineralogy, Petrology and Geochemistry* 19, 305-309 (in Chinese with English abstract).
- Mirnejad H., Simonetti A., Molasalehi F., 2011. Pb isotopic compositions of some Zn-Pb deposits and occurrences from Urumieh-Dokhtar and Sanandaj-Sirjan zones in Iran. *Ore Geology Review* 39, 181-187.
- Modaberi S., 1994. Geology, facies analysis, mineralogy, geochemistry and genesis of the Ravanj-Delijan Pb-Ag deposit. Unpublished M.Sc. thesis, Tehran, Tarbiat Modares University.
- Mohajjel M., Fergusson C.L., Sahandi M.R., 2003. Cretaceous-Tertiary convergence and continental collision, Sanandaj-Sirjan zone, western Iran. *Journal of Asian Earth Sciences* 21, 397-412.
- Momenzadeh M., 1976. Stratabound lead-zinc ores in the lower Cretaceous and Jurassic sediments in the Malayer-Esfahan district (west central Iran), lithology, metal content, zonation and genesis. Unpublished Ph.D. thesis, Heidelberg, University of Heidelberg, 300 pp.
- Ohmoto H., 1972. Systematics of the sulfur and carbon in hydrothermal ore deposits. *Economic Geology* 67, 551-579.
- Ohmoto H. and Goldhaber M.B., 1997. Sulfur and carbon isotopes. In: *Geochemistry of Hydrothermal ore Deposits*. (Ed.): H.L. Barnes, John Wiley and Sons, New York, 517-611.
- Ohmoto H. and Rye R.O., 1979. Isotopes of sulfur and carbon. In: *Geochemistry of Hydrothermal Ore Deposits*. (Ed.): H.L. Barnes, Wiley, New York, 509-567.
- Rajabi A., Rastad E., Canet C., 2012. Metallogeny of Cretaceous carbonate-hosted Zn-Pb deposits of Iran: geotectonic setting and data integration for future mineral exploration. *International Geology Review* 54, 1649-1672.
- Rastad E., 1981. Geological, mineralogical and ore facies investigations on the Lower Cretaceous stratabound Zn - Pb - Ba - Cu deposits of the Irankuh mountain range, Isfahan, west central Iran. Ph.D. thesis, Heidelberg University, Heidelberg, Germany, 334 pp.
- Reichert J., 2007. A metallogenic model for carbonate-hosted non-sulphide zinc deposits based on observations of Mehdi Abad and Irankuh, Central and Southwestern Iran. Ph.D thesis, Martin Luther University Halle Wittenberg, Halle, Germany, 152 pp.
- Roedder E., 1972. The composition of fluid inclusions. In: *US Geological Survey Professional Paper*, 164 pp.
- Roedder E., 1984. Fluid inclusions. In: *Reviews in Mineralogy* 12. Mineralogical Society of America, Washington, DC, 644 pp.
- Şengör A., 1990. A new model for the late Palaeozoic-Mesozoic tectonic evolution of Iran and implications for Oman. *Geological Society, London, Special Publications*, 49, 797-831.
- Shepherd T.J., Rankin A.H., Alderton D.H.M., 1985. A practical guide to fluid inclusion studies. London, UK, Blackie.
- Shufeng Y.J., Chengzao C., Hanlin W., Guoqi C., Jia X., Xiao D., Guo S., 2002. Tectonic evolution of Tethyan tectonic field, formation of Northern Margin basin and explorative

- perspective of natural gas in Tarim Basin. *Chinese Science Bulletin* 47, 34-46.
- Saboori M., Karimpour M.H., Malekzadeh Shafaroudi A., 2019. Mineralogy, ore chemistry, and fluid inclusion studies in Gushfil Pb-Zn deposit, Irankuh mining district, SW Isfahan. *Iranian Journal of Crystallography and Mineralogy* 26, 857-870. (In Persian with English abstract).
- Sangster D.F., 1990. Mississippi Valley-type and Sedex lead-zinc deposits: a comparative examination. *Trans. Inst. Min. Metall., Sect. B, Applied Earth Sciences* 99, 21-42.
- Seal II R.R., 2006. Sulfur isotope geochemistry of sulfide minerals. *Reviews in Mineralogy and Geochemistry* 61, 633-677.
- Stacey J.S. and Kramers J.D., 1975. Approximation of terrestrial lead isotope evolution by a two-stage model. *Earth Planetary Science Letter* 26, 207-221.
- Steele-MacInnis M, Lecumberri-Sanchez P, Bodnar R.J., 2012. HokieFlincs-H₂O-NaCl: A Microsoft Excel spreadsheet for interpreting microthermometric data from fluid inclusions based on the PVTX properties of H₂O-NaCl. *Computers and Geosciences* 49, 334-337.
- Van den Kerkhof A.M. and Hein U., 2001. Fluid inclusion petrography. *Lithos* 55, 27-47.
- White W.M., 2013. *Geochemistry*. Wiley-Blackwell, Oxford, 672 pp.
- Whitney D.L. and Evans B.W., 2010. Abbreviations for names of rock-forming minerals. *American Mineralogist* 95, 185-187.
- Zahedi M., 1976. Explanatory Text of the Isfahan Quadrangle Map:1:250,000; Geological Quadrangle F8. Geological Survey of Iran, Tehran, Iran.
- Zartman R.E. and Doe B.R., 1981. Plumbotectonics - the model. *Tectonophysics* 75, 135-162.
- Zartman R.E. and Haines S.M., 1988. The plumbotectonic model for Pb isotopic systematics among major terrestrial reservoirs - a case for bidirectional transport. *Geochimica et Cosmochimica Acta* 52, 1327-1339.



This work is licensed under a Creative Commons Attribution 4.0 International License CC BY. To view a copy of this license, visit <http://creativecommons.org/licenses/by/4.0/>